Mass-independent fractionation of sulfur isotopes in sulfides from the pre-3770 Ma Isua Supracrustal Belt, West Greenland

D. PAPINEAU* AND S. J. MOJZSIS

Department of Geological Sciences and Center for Astrobiology, University of Colorado, UCB0399, Boulder, CO 80309, USA

ABSTRACT

Redox chemistry of the coupled atmosphere–hydrosphere system has coevolved with the biosphere, from global anoxia in the Archean to an oxygenated Proterozoic surface environment. However, to trace these changes to the very beginning of the rock record presents special challenges. All known Eoarchean (*c.* 3850–3600 Ma) volcanosedimentary successions (i.e. supracrustal rocks) are restricted to high-grade gneissic terranes that seldom preserve original sedimentary structures and lack primary organic biomarkers. Although complicated by meta-morphic overprinting, sulfur isotopes from Archean supracrustal rocks have the potential to preserve signatures of both atmospheric chemistry and metabolic fractionation from the original sediments. We present a synthesis of multiple sulfur isotope measurements (^{32}S, ^{33}S and ^{34}S) performed on sulfides from amphibolite facies banded iron-formations (BIFs) and ferruginous garnet-biotite (metapelitic) schists from the pre-3770 Ma Isua Supracrustal Belt (ISB) in West Greenland. Because these data come from some of the oldest rocks of interpretable marine sedimentary origin, they provide the opportunity to (i) explore for possible biosignatures of sulfur metabolisms in early life; (ii) assess changes in atmospheric redox chemistry from ~3.8 Ga; and (iii) lay the groundwork to elucidate sulfur biogeochemical cycles on the early Earth. We find that sulfur isotope results from Isua do not unambiguously indicate microbially induced sulfur isotopic fractionation at that time. A significantly expanded data set of Δ^{33}S analyses for Isua dictates that the atmosphere was devoid of free oxygen at time of deposition and also shows that the effects of post-depositional metamorphic remobilization and/or dilution can be traced in mass-independently fractionated sulfur isotopes.

Corresponding author: D. Papineau. Tel.: 202-478-8917; fax: 202-478-8901; e-mail: dpapineau@ciw.edu.

INTRODUCTION

The oldest known terrestrial rocks of sedimentary origin (~3.8 Ga) are often strongly deformed and have been extensively metamorphosed during several thermal events (reviewed in Nutman *et al.*, 2004). The only means to directly investigate the emergence of the biosphere on the early Earth is through the development and recognition of biosignatures for such rocks. Because the oldest terranes have endured protracted metamorphic histories, different interpretations have been proposed for stable isotope data used in the search for early life. Over the years, evidence for and against relict traces of an early microbial biosphere preserved in the pre-3770 Ma rocks of the Isua Supracrustal Belt (ISB) of West

Greenland has been offered. Controversies largely stem from different interpretations of protoliths to the studied supracrustal units (reviewed in Friend *et al.*, 2002 and Myers, 2002), e.g. are they sedimentary or the result of metamorphic processes on originally igneous rocks? Other conflicting views of possible biological signatures vs. abiological effects that mimic such signatures in the ISB concern carbon isotope ratios from graphitic matter (Schidlowski, 1988; Mojzsis *et al.*, 1996; Rosing, 1999; van Zuilen *et al.*, 2002) and nitrogen isotopes from carbonate veins and garnet–biotite schists (Pinti *et al.*, 2001; Papineau *et al.*, 2005b; van Zuilen *et al.*, 2005). Rocks of sedimentary protolith, such as banded iron-formations (BIF) and garnet–biotite schists of probable ferruginous pelitic origin (clay-rich sedimentary protoliths) are recognizable throughout the ISB. Because these rocks are of marine sedimentary origin (Dymek & Klein, 1988) they are important candidate materials to host information relevant to the geobiology of the Eoarchean oceans. In line

*Present address: Geophysical Laboratory, Carnegie Institution of Washington, 5251 Broad Branch Road, NW, Washington DC 20015, USA.

with these observations, it was proposed some time ago that sulfur isotopes in sulfides from the metamorphic equivalents of pelagic sedimentary rocks could preserve isotopic evidence of the early biosphere (Monster *et al.*, 1979; Schidlowski *et al.*, 1983). Detection and identification of geochemical clues that shed light on the origin of sulfur metabolisms in the ancient rock record is essential to determine both the time of the emergence of early metabolic pathways and to place direct constraints on the environmental conditions in which they evolved.

Metabolic reactions that involve sulfur compounds are an ancient feature of life and could in principle be recorded by characteristic sulfur isotope fractionations in the oldest sedimentary rocks. This possibility arises from the observation that some of the most deeply branching lineages of Bacteria and Archaea in the phylogenetic tree based on small subunit ribosomal RNA (ssu rRNA) can metabolize sulfur compounds (Stetter & Gaag, 1983). Importantly, there is no known relationship between the phylogenetic position (based on ssu rRNA) of organisms that carry out microbial sulfate reduction (MSR) and the magnitude to which sulfur isotopes are fractionated (Detmers *et al.*, 2001). Biological reduction of sulfate to sulfide often produces significant sulfur isotope fractionation because $^{32}SO_4^{2-}$ is preferentially reduced compared to $^{34}SO_4^{2-}$, and the product H_2S can be depleted in ^{34}S by up to 46‰ when sulfate is nonlimited (Canfield & Raiswell, 1999; references therein). Aqueous sulfate concentrations and other factors can influence the magnitude of isotopic fractionation during MSR such that sulfate concentrations inferior to 200 µM are not conducive to significant sulfur isotope fractionation (Habicht *et al.*, 2002). Sedimentary sulfides preserve a large range of $^{34}S/^{32}S$ ratios, and this range appears to have gradually increased over geological time (Canfield, 1998). The progressive increase is consistent with the step-wise accumulation of seawater sulfate in periods of significant atmospheric oxygen accumulation in the Paleo- and Neoproterozoic. Such environmental changes likely favored the population expansion of microbial sulfate reducers, which would have contributed to the observed increase in the range of sulfur isotope ratios in the Palaeoproterozoic (Canfield & Raiswell, 1999).

In an anoxic atmosphere, mass-independently fractionated (MIF) sulfur is produced from ultraviolet photochemical reactions on sulfur-containing gases, and the signature of this effect can be preserved in sedimentary sulfide and sulfate minerals (Farquhar *et al.*, 2000). Archean sedimentary sulfides and sulfates often have $\Delta^{33}S$ values beyond the range of −0.30 to +0.30‰ often used to describe mass-dependent fractionation (MDF) processes, and uphold other evidence for the absence of significant atmospheric oxygen before 2.5 Ga (Farquhar *et al.*, 2000; Hu *et al.*, 2003; Mojzsis *et al.*, 2003; Ono *et al.*, 2003; Whitehouse *et al.*, 2005). However, as a consequence of limited exposure and difficult access to samples, relatively few studies have focused exclusively on the sulfur isotope composition of sulfide or sulfate from Eoarchean sedimentary rocks. Bulk sulfides from *c.* 3.77 Ga Isua (West Greenland) BIFs have $\delta^{34}S$ values in the range of −1.0 to +2.0‰, comparable to values measured from associated garnet–amphibolite rocks of basaltic composition (Monster *et al.*, 1979) that volumetrically dominate the lithotypes preserved in the ISB. Similar $\delta^{34}S$ values for pyrite in other BIF units from Isua range between −1.2 to +2.5‰ and were interpreted by Strauss (2003) to reflect magmatic and hydrothermal processes in the sulfur cycle with no apparent biological fractionation. The objectives of this study were to search for chemical features of the atmosphere/hydrosphere system at Isua time, to explore for evidence of early sulfur metabolisms and to trace the fate of MIF sulfur isotopes in highly metamorphosed sediments. The latter objective is important because variations of $\Delta^{33}S$ values in BIFs may be related to metamorphic history and the possible migration or dilution of MIF sulfur isotopes by later fluid alterations at Isua (e.g. Rose *et al.*, 1996). We used high-resolution secondary ion mass spectrometry in multicollection mode to explore the distribution of $\Delta^{33}S$ values in sulfide microdomains of selected BIF and garnet–biotite schist samples to trace processes responsible for the modification of sulfur isotope signatures. We report 54 analyses of multiple sulfur isotopes from eight separate rock samples, which significantly expand the current inventory of published $\Delta^{33}S$ data from Isua metasedimentary rocks.

Sample description

The ISB in West Greenland is part of the Eoarchean (3.85–3.6 Ga) Itsaq Gneiss Complex (Nutman *et al.*, 1996) and forms an arcuate belt approximately 35 km long. The ISB has historically been divided by workers in the field into an eastern and western 'section' (Fig. 1). It is a volcanosedimentary (supracrustal) sequence that broadly resembles other younger Archean granite + 'greenstone' gneiss terranes. What sets it apart is that it is ancient (>3.7 Ga) and has been extensively deformed and metamorphosed up to amphibolite facies, such that the amphibolites are black and often garnetiferous. Some units also show evidence for intense local metasomatism, silicification, carbonatization and major element remobilization (Rose *et al.*, 1996). For instance, alkali metasomatism and interaction with CO_2-rich fluids appear to have affected most rock types in the ISB, which has led to the suggestion that carbonate-rich garnet + hornblende + biotite schists formed from the *in situ* replacement of amphibolite protoliths (Rosing *et al.*, 1996). In the last decade, reliable age constraints for the ISB have been determined by ion microprobe U-Pb analyses on zircons from adjacent orthogneisses and from rocks assigned a felsic volcanic origin in the Itsaq Gneiss Complex; ages for these vary between 3.7 and 3.8 Ga (reviewed Nutman *et al.*, 1996). The post-depositional history of the ISB appears to have included a ~3.65 Ga high-grade metamorphic event perhaps related to tectonic collisions (reviewed in Friend & Nutman, 2005), granitoid intrusions around 3.14 Ga and a
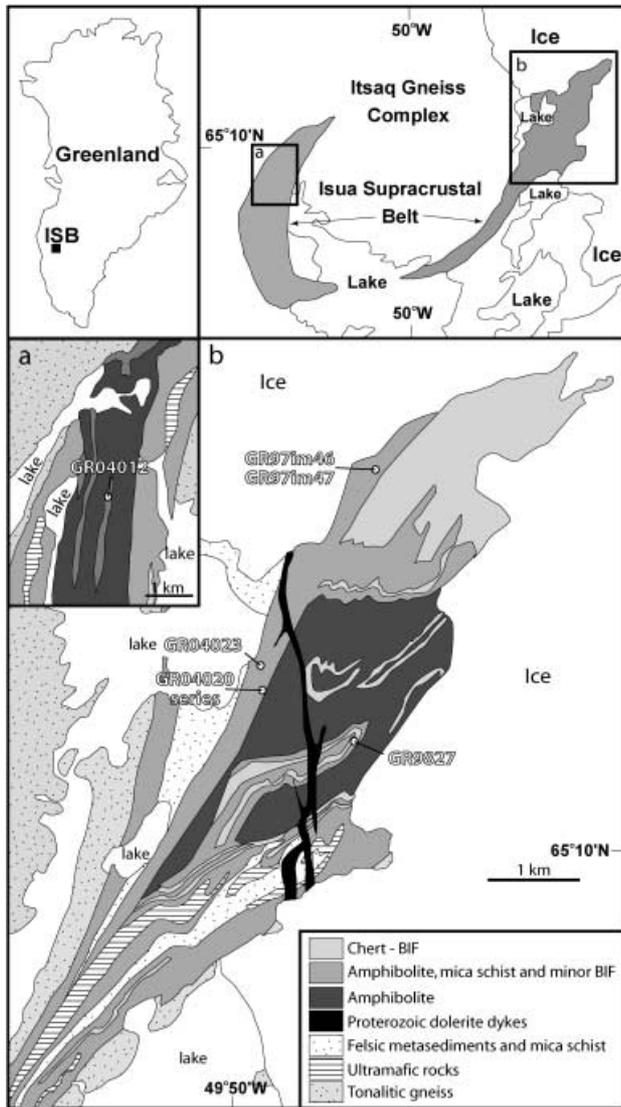
Fig. 1 Simplified geological map of the north-east section of the Isua Supracrustal Belt in south-west Greenland showing the location of samples analysed in this study (modified from Myers, 2001).

several other metamorphic events during the Late Archean and Paleoproterozoic (Nutman *et al.*, 1996). Considerable debate lingers over the interpretation of some protoliths to the ISB suite, and the controversies have focused on the origin of metavolcanic and metamorphosed clastic rocks (e.g. Fedo *et al.*, 2001) as well as on the importance and prevalence of metasomatized units. Rocks in the ISB for which protolith assignments are accepted by most workers include pillow lavas (garnet amphibolites), BIFs (magnetite-bearing banded quartzites) and metapelites (ferruginous garnet–biotite schists). Despite the variable strain, in some low-strain halos it can be established that these rock types occur in conformable contact to each other, which suggests that they formed at the same time and in similar environments.

We investigated three rocks of probable clay-rich sedimentary origin and five BIF samples from Isua. Sample localities are shown in Fig. 1 and a brief description of each is given in Table 1. Samples *GR97im46* and *GR97im47* are quartz–biotite–garnet schists collected approximately 2 m apart from an outcrop of the 'Sequence B2' mica schist of Nutman *et al.* (1984). The schists contain cm-scale quartz lenses generally orientated parallel to schistosity defined by the dominant biotite + garnet mineralogy. Published sulfur isotope analyses of anhedral pyrite (FeS_2) that occur as interstitial blebs in biotite from sample *GR97im43* (collected within 5 m of *GR97im46*) showed positive $\Delta^{33}S$ values between +1.10 and +1.23‰ as well as a small range of $\delta^{34}S$ between −0.9 and +0.7‰ (Mojzsis *et al.*, 2003). To investigate the mobility of sulfur in this rock we analysed chalcopyrite ($CuFeS_2$) and cubanite ($CuFe_2S_3$) grains found only within the quartz lenses of samples *GR97im46* and *GR97im47*; the lenticular quartz components are probably deformed veins and therefore later components to the schists. Sample *GR04023* is a garnet-bearing mica schist that contains chalcopyrite and pyrrhotite collected ~2 km south and along strike of the *im*-series. The sample came from a deformed unit cross-cut by an amphibolitized doleritic dyke ascribed to the Ameralik dike swarm of the Itsaq Gneiss Complex. BIF sample *GR9827* was collected from an outcrop visibly rich in sulfur and most likely affected by pervasive post-depositional sulfide-rich metamorphic fluids, which also sulfidized other nearby rocks. Sample *GR9827* was

Table 1 Brief description of samples analysed for sulfur isotopes

Sample name*	GPS coordinates	Rock type	Mineralogy[†]	Sulfide phase[†]
GR97im46	N65°11′53.2″ W49°48′14.8″	Metapelite	Qtz + Bt + Grt – Plag – Mgt – Su	Cu
GR97im47	N65°11′53.2″ W49°48′14.8″	Metapelite	Qtz + Bt + Grt – Plag – Gru – All – Su	Ch, Cu
GR9827	N65°10′31.6″ W49°48′02.5″	BIF	Qtz + Mgt + Gru – Su	Py
GR04012	N65°08′44.8″ W50°10′14.3″	BIF	Qtz + Mgt + Gru + Bt + Chl – Su	Po
GR04020-80	N65°10′17.4″ W49°48′52.9″	BIF	Qtz + Mgt + Gru – Bt – Su	Py
GR04020-120	N65°10′17.4″ W49°48′52.9″	BIF	Qtz + Mgt + Gru – Bt – Su	Py
GR04020-160	N65°10′17.4″ W49°48′52.9″	BIF	Qtz + Mgt + Gru – Bt – Su	Py
GR04023	N65°10′27.8″ W49°49′25.9″	Metapelite	Qtz + Grt + Bt + Ilm – Su	Ch, Po

[†]Mineral abbreviations: All, allanite; Bt, biotite; Ch, chalcopyrite; Chl, chlorite; Cu, cubanite; Grt, garnet; Gru, grunerite; Ilm, ilmenite; Mgt, magnetite; Plag, plagioclase; Po, pyrrhotite; Py, pyrite; Qtz, quartz; Su, sulfides. Mostly after Kretz (1983).

Table 2 WDS analyses of the chemical composition of analysed Isua sulfides

Analysed sulfides*	Fe	S	Co	Ni	Cu	Zn	Total	Phase
GR97im46a	37.14	34.42	0.0707	0.0204	22.02	0.0150	93.68	Cu
GR97im46b	37.41	35.08	0.0408	0.0000	22.40	0.0479	94.98	Cu
GR97im46c	37.84	35.67	0.0110	0.0032	23.19	0.0479	96.75	Cu
GR97im46d	38.56	35.62	0.0000	0.0000	23.28	0.0055	97.47	Cu
GR97im46e	39.36	35.64	0.0000	0.0000	23.72	0.0574	98.78	Cu
GR97im46f	37.99	36.64	0.0389	0.0000	22.84	0.0671	97.57	Cu
GR97im46g	38.46	35.21	0.0745	0.0000	23.75	0.0137	97.51	Cu
GR97im47a	38.37	33.26	0.0515	0.0000	23.55	0.0000	95.23	Cu
GR97im47b	38.95	35.75	0.0844	0.0461	23.78	0.0136	98.62	Cu
GR97im47c	28.67	35.54	0.0000	0.0562	35.51	0.0514	99.84	Ch
GR97im47d	28.42	34.53	0.0000	0.0000	34.49	0.0279	97.46	Ch
GR9827a	45.82	53.88	0.0252	0.0192	0.0194	0.0000	99.76	Py
GR9827b	45.82	54.27	0.0759	0.0173	0.0000	0.0000	100.18	Py
GR9827c	45.82	54.54	0.0156	0.0203	0.0721	0.0299	100.50	Py
GR9827d	45.71	54.22	0.0664	0.0163	0.0000	0.0000	100.02	Py
GR9827e	46.22	53.75	0.0537	0.0102	0.0441	0.0000	100.08	Py
GR9827f	45.68	54.42	0.0812	0.0000	0.0233	0.0000	100.21	Py
GR04012e	59.02	40.05	0.0370	0.1651	0.1270	0.0143	99.41	Po
GR04012f	59.40	39.20	0.1024	0.2390	0.0645	0.0000	99.01	Po
GR04020_80a	47.75	55.09	0.0341	0.0000	0.0000	0.0198	102.90	Py
GR04020_80b	47.30	54.83	0.0426	0.0912	0.1015	0.0000	102.37	Py
GR04020_80c	46.40	55.16	0.7912	0.0278	0.0241	0.0226	102.43	Py
GR04020_80d	46.52	54.91	0.5925	0.0356	0.0254	0.0113	102.10	Py
GR04020_120a	46.40	54.19	0.0421	0.2005	0.0052	0.0137	100.85	Py
GR04020_120b	46.97	54.13	0.0390	0.0664	0.0231	0.0000	101.23	Py
GR04020_120c	46.77	54.88	0.1689	0.0320	0.0000	0.0354	101.88	Py
GR04020_120d	47.06	54.91	0.1401	0.0544	0.0231	0.0558	102.24	Py
GR04020_120e	46.27	55.40	0.0798	0.0277	0.0359	0.0368	101.85	Py
GR04020_120f	46.65	54.70	0.1602	0.1054	0.0000	0.0000	101.61	Py
GR04020_120g	45.97	54.67	0.1957	0.0053	0.0000	0.0149	100.85	Py
GR04020_160a	46.93	54.61	0.3176	0.0342	0.0435	0.0000	101.94	Py
GR04023a	30.00	35.37	0.0357	0.0467	36.36	0.0244	101.84	Ch
GR04023b	29.49	35.03	0.0000	0.0000	36.24	0.2584	101.02	Ch
GR04023c	29.66	35.66	0.0377	0.0000	36.36	0.0068	101.72	Ch
GR04023d	58.64	40.20	0.0147	0.0055	0.0885	0.0000	98.95	Po
GR04023f	56.40	40.57	0.0944	0.7425	0.0000	0.0000	97.80	Po

*Nomenclature for the analysed sulfides is the sample name followed by a letter, which indicates the specific sulfide grain in the thin section.

analysed to trace the source of sulfur and possible mixing of sulfur isotopes in metamorphic fluids that played a role in the sulfidization endemic to the outcrop. Three samples of the *GR04020*-series came from the same outcrop of finely laminated BIF *GR97im23* described in Mojzsis *et al.* (2003) in the north-east sector of the ISB. The samples were collected at up-section distances of 80, 120 and 160 cm away from the original sample site of *GR97im23*. Sulfides were analysed to search for possible variations of $\Delta^{33}S$ and/or $\delta^{34}S$ at the outcrop scale in this well-preserved BIF unit. An additional BIF sample *GR04012* was collected from a relatively weathered outcrop intercalated with garnet–mica schists in the western sector of the ISB for purposes of comparison with other BIFs from the eastern limb of the belt.

METHODS AND RESULTS

Optically polished 2.5-cm-diameter round thin sections were prepared, and sulfide grains were mapped in transmitted and reflected light prior to wavelength dispersive spectroscopy (WDS) following the methods described in Greenwood *et al.* (2000). Results for sulfide chemistry (S, Fe, Cu, Co, Ni and Zn) from WDS analyses are detailed in Table 2 and we note that these did not reveal unusual amounts of Co, Ni or Zn in the sulfide phases analysed. These preparatory steps allowed us to be selective in the targets for isotope analyses by ion microprobe. Data collection was performed following our usual procedures (Mojzsis *et al.*, 2003; Papineau *et al.*, 2005a) and was part of a larger analytical session in May 2005 (Session 2 of Papineau *et al.* submitted). The overall reported 2 σ error on delta values is twice the quadratic of the internal and external errors, which in all cases is dominated by the latter. Analyses on standards were calculated using York regression and plotted on a slope of λ = 0.5184 ± 0.0049 (2 σ). Because it has been documented that MIF sulfur isotopes can be heterogeneously distributed within individual grains (Mojzsis *et al.*, 2003), when possible we performed multiple spot analyses on individual sulfides.
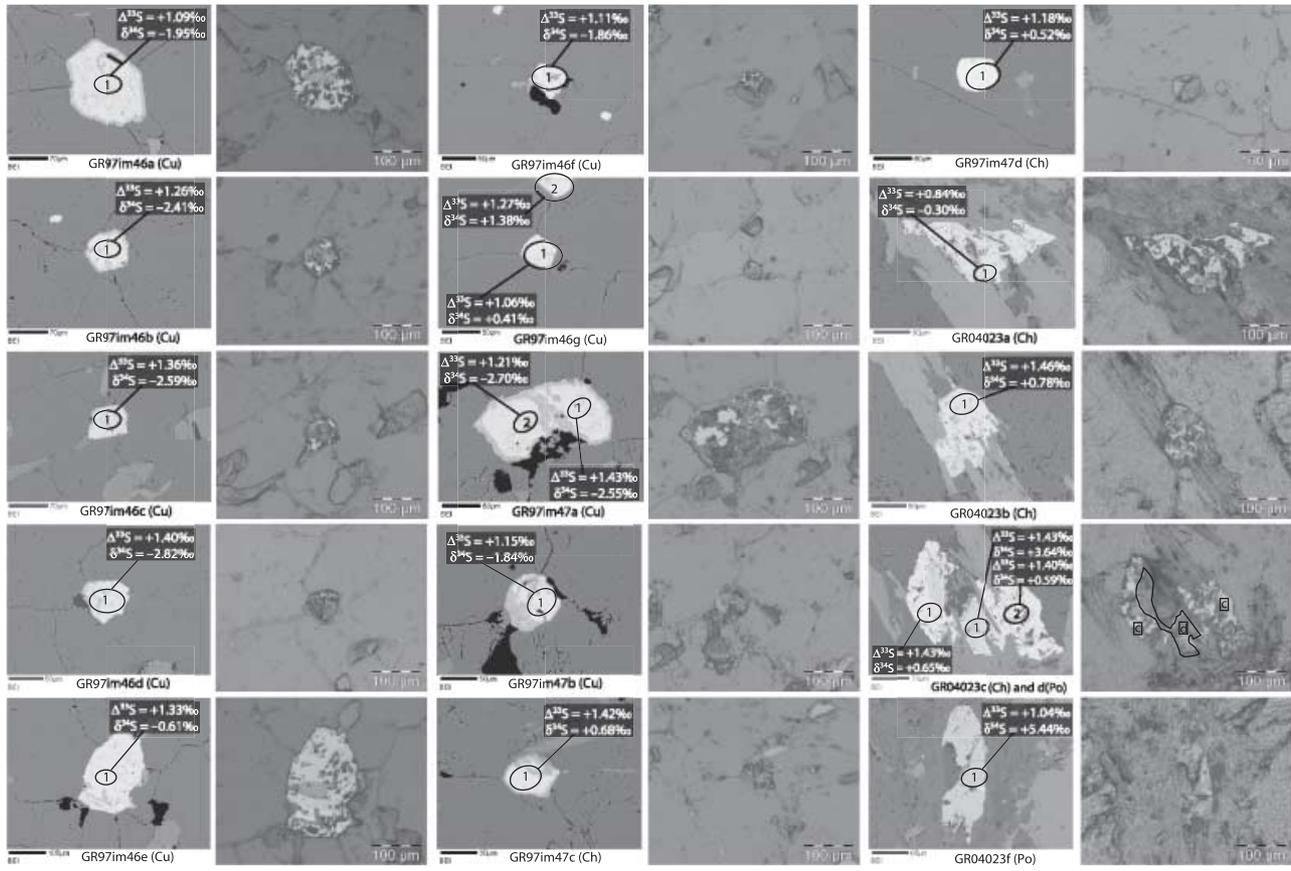
Fig. 2 Three sets of columns of backscattered electron images (left columns) and transmitted/reflected light images (right columns) of sulfides analysed from metapelite samples *GR97im46*, *GR97im47* and *GR04023*. Ion microprobe spots are shown along with the measured δ^{34}S and Δ^{33}S values.

Garnet–biotite schist (metapelite) samples

Backscattered electron and reflected/transmitted light images of individual sulfides analyzed from metapelitic schist samples are shown in Fig. 2. To avoid sample-to-sample changes in the geometry of individual mounts in the ion microprobe sample chamber that can affect instrumental mass fractionation for sulfur isotopes (e.g. Papineau *et al.*, 2005a), we prepared mounts that contained pre-cut selected sulfide-rich portions of polished thin sections from *GR97im47* and *GR97im46* cast along with standard grains on the same mount. Samples *GR97im47* and *GR97im46* contained cubanite, a phase with known occurrences in high-temperature hydrothermal deposits (Anthony *et al.*, 1990). Because at the time of our analysis no cubanite standard was available, we provisionally assumed a chalcopyrite behaviour for instrumental mass fractionation (IMF) correction, the calculation of delta-values and for error analysis. Cubanite and chalcopyrite have stoichiometrically identical proportions of S and [Fe + Cu]. Because of their similar chemical compositions and the insignificant difference in average ^{32}S intensities measured between cubanite and chalcopyrite (Table 3), we consider the effect of using our

chalcopyrite standard to correct for IMF rather than the true phase as minimal, but acknowledge that a small related error be kept in mind. It is important to point out that such phase effects between chalcopyrite and cubanite on IMF correction may be significant for mass-dependent behaviour, but they are not relevant for Δ^{33}S values beyond the range of MDF. The analysed cubanite and chalcopyrite are in coarse-grained quartz lenses of probable late origin in both *GR97im46* and *GR97im47* and are subhedral to anhedral in habit with thin rims of Fe-oxide from recent oxidative weathering. Analyses are presented in a three-isotope plot in Fig. 3 where Δ^{33}S values are between +1.06 and +1.43‰ and δ^{34}S between −2.82 and +1.38‰ (Table 3). These results are consistent with previously reported sulfur isotope data for anhedral pyrites in *GR97im43* with Δ^{33}S values between +1.10 and +1.23‰ (Mojzsis *et al.*, 2003). Garnet–mica schist sample *GR04023* was collected about 2 km south and along strike of the outcrop of the *im*-series and revealed similar sulfur isotopic composition. Subhedral grains of chalcopyrite and pyrrhotite surrounded by quartz + biotite and close to large (>400 μM) poikilitic garnet crystals in *GR04023* have Δ^{33}S values between +0.83 and +1.46‰ and δ^{34}S values between −0.30

Table 3 Sulfur isotope analyses of sulfides from Isua metasediments

Grain spot*	$^{34}S/^{32}S$	±1 σ	$^{33}S/^{32}S$	±1 σ	^{32}S average intensity	$\delta^{34}S_{CDT}$ (‰)	±2 σ[†] (‰)	$\delta^{33}S_{CDT}$ (‰)	±2 σ[†] (‰)	$\Delta^{33}S$ (‰)	±2 σ[†] (‰)
GR97im46a@1	4.4077E-02	1.20E-06	7.8840E-03	6.51E-07	4.94E+08	−1.95	0.98	+0.08	0.55	+1.09	0.24
GR97im46b@1	4.4056E-02	1.04E-06	7.8835E-03	7.60E-07	4.87E+08	−2.41	0.97	+0.01	0.56	+1.26	0.26
GR97im46c@1	4.4048E-02	1.77E-06	7.8835E-03	6.55E-07	5.09E+08	−2.59	0.98	+0.02	0.55	+1.36	0.24
GR97im46d@1	4.4038E-02	1.80E-06	7.8829E-03	4.39E-07	4.86E+08	−2.82	0.98	−0.06	0.54	+1.40	0.21
GR97im46e@1	4.4136E-02	1.24E-06	7.8914E-03	5.77E-07	4.77E+08	−0.61	0.98	+1.01	0.55	+1.33	0.23
GR97im46f@1	4.4080E-02	1.73E-06	7.8846E-03	1.03E-06	2.78E+08	−1.86	0.98	+0.15	0.59	+1.11	0.32
GR97im46g@1	4.4181E-02	1.88E-06	7.8934E-03	1.30E-06	2.25E+08	+0.41	0.98	+1.27	0.62	+1.06	0.37
GR97im46g@2	4.4224E-02	1.95E-06	7.8990E-03	1.52E-06	2.73E+08	+1.38	0.98	+1.98	0.65	+1.27	0.42
GR97im47a@1	4.4050E-02	1.35E-06	7.8843E-03	8.65E-07	4.21E+08	−2.55	0.98	+0.11	0.57	+1.43	0.28
GR97im47a@2	4.4044E-02	2.75E-06	7.8819E-03	1.22E-06	1.89E+08	−2.70	0.98	−0.19	0.61	+1.21	0.36
GR97im47b@1	4.4081E-02	2.28E-06	7.8849E-03	8.59E-07	3.64E+08	−1.84	0.98	+0.20	0.57	+1.15	0.28
GR97im47c@1	4.4193E-02	2.03E-06	7.8974E-03	7.28E-07	3.69E+08	+0.68	0.98	+1.78	0.56	+1.42	0.26
GR97im47d@1	4.4186E-02	1.66E-06	7.8949E-03	7.45E-07	3.64E+08	+0.52	0.98	+1.45	0.56	+1.18	0.26
GR9827a@1	4.4120E-02	1.17E-06	7.8808E-03	5.45E-07	5.51E+08	−0.97	0.98	−0.34	0.54	+0.17	0.23
GR9827b@1	4.4060E-02	8.13E-07	7.8760E-03	6.37E-07	5.70E+08	−2.31	0.97	−0.94	0.55	+0.26	0.24
GR9827c@1	4.4091E-02	1.03E-06	7.8784E-03	4.00E-07	5.45E+08	−1.63	0.97	−0.64	0.54	+0.21	0.20
GR9827c@2	4.4103E-02	1.10E-06	7.8795E-03	5.57E-07	5.48E+08	−1.35	0.97	−0.49	0.55	+0.21	0.23
GR9827c@3	4.4156E-02	9.35E-07	7.8840E-03	6.43E-07	5.27E+08	−0.15	0.97	+0.07	0.55	+0.15	0.24
GR9827c@4	4.4109E-02	1.09E-06	7.8801E-03	4.76E-07	5.25E+08	−1.21	0.97	−0.42	0.54	+0.21	0.21
GR9827d@1	4.4098E-02	1.24E-06	7.8794E-03	6.85E-07	4.53E+08	−1.46	0.98	−0.50	0.55	+0.25	0.25
GR9827d@2	4.4095E-02	1.01E-06	7.8778E-03	5.92E-07	5.23E+08	−1.53	0.97	−0.70	0.55	+0.09	0.23
GR9827e@1	4.4213E-02	3.25E-06	7.8924E-03	2.37E-06	1.78E+08	+1.14	0.98	+1.14	0.80	+0.55	0.63
GR9827f@1	4.4211E-02	1.67E-06	7.8885E-03	1.15E-06	2.43E+08	+1.11	0.98	+0.64	0.60	+0.07	0.34
GR9827f@2	4.4176E-02	1.96E-06	7.8869E-03	8.81E-07	2.75E+08	+0.31	0.98	+0.45	0.57	+0.29	0.29
GR04012e@1	4.4281E-02	1.61E-06	7.9044E-03	8.34E-07	2.76E+08	+2.67	0.98	+2.67	0.57	+1.28	0.28
GR04012e@2	4.4256E-02	2.07E-06	7.9015E-03	1.32E-06	1.88E+08	+2.11	0.98	+2.30	0.62	+1.21	0.38
GR04012f@1	4.4228E-02	3.19E-06	7.8992E-03	2.97E-06	7.12E+07	+1.49	0.98	+2.01	0.92	+1.24	0.77
GR04020_80a@1	4.4160E-02	1.30E-06	7.9008E-03	6.49E-07	5.01E+08	−0.07	0.98	+2.20	0.55	+2.24	0.24
GR04020_80b@1	4.4173E-02	9.92E-07	7.9023E-03	4.70E-07	5.45E+08	+0.23	0.97	+2.39	0.54	+2.27	0.21
GR04020_80b@2	4.4147E-02	1.03E-06	7.8983E-03	6.87E-07	5.52E+08	−0.36	0.97	+1.89	0.55	+2.08	0.25
GR04020_80b@3	4.4178E-02	1.27E-06	7.9026E-03	5.15E-07	5.54E+08	+0.35	0.98	+2.43	0.54	+2.25	0.22
GR04020_80c@1	4.4166E-02	1.21E-06	7.9023E-03	5.39E-07	5.45E+08	+0.08	0.98	+2.40	0.54	+2.36	0.22
GR04020_80d@1	4.4174E-02	1.12E-06	7.9028E-03	6.76E-07	5.62E+08	+0.26	0.97	+2.46	0.55	+2.33	0.25
GR04020_80d@2	4.4168E-02	1.20E-06	7.9008E-03	6.83E-07	5.52E+08	+0.12	0.98	+2.21	0.55	+2.14	0.25
GR04020_80d@3	4.4175E-02	1.25E-06	7.9022E-03	4.89E-07	5.56E+08	+0.29	0.98	+2.39	0.54	+2.24	0.22
GR04020_80d@4	4.4169E-02	9.45E-07	7.9023E-03	5.77E-07	5.30E+08	+0.15	0.97	+2.39	0.55	+2.32	0.23
GR04020_80d@5	4.4186E-02	1.22E-06	7.9033E-03	5.76E-07	5.44E+08	+0.52	0.98	+2.52	0.55	+2.25	0.23
GR04020_120a@1	4.4149E-02	1.09E-06	7.9002E-03	5.85E-07	5.03E+08	−0.32	0.97	+2.14	0.55	+2.30	0.23
GR04020_120b@1	4.4155E-02	7.41E-07	7.9006E-03	5.82E-07	5.55E+08	−0.18	0.97	+2.18	0.55	+2.28	0.23
GR04020_120c@1	4.4274E-02	1.32E-06	7.9112E-03	7.07E-07	4.10E+08	+2.53	0.98	+3.53	0.56	+2.22	0.25
GR04020_120d@1	4.4225E-02	1.25E-06	7.9058E-03	6.66E-07	4.61E+08	+1.41	0.98	+2.84	0.55	+2.10	0.25
GR04020_120e@1	4.4173E-02	1.05E-06	7.9022E-03	4.10E-07	5.54E+08	+0.24	0.97	+2.38	0.54	+2.26	0.21
GR04020_120e@2	4.4176E-02	9.31E-07	7.9033E-03	3.96E-07	5.52E+08	+0.29	0.97	+2.53	0.54	+2.38	0.20
GR04020_120f@1	4.4161E-02	1.04E-06	7.9018E-03	5.05E-07	5.61E+08	−0.04	0.97	+2.33	0.54	+2.35	0.22
GR04020_120f@2	4.4174E-02	1.12E-06	7.9035E-03	5.70E-07	5.56E+08	+0.25	0.97	+2.55	0.55	+2.42	0.23
GR04020_120g@1	4.4167E-02	1.22E-06	7.9025E-03	5.59E-07	5.61E+08	+0.09	0.98	+2.42	0.55	+2.37	0.23
GR04020_160a@1	4.4136E-02	9.91E-07	7.8994E-03	6.13E-07	5.26E+08	−0.60	0.97	+2.03	0.55	+2.34	0.24
GR04020_160a@2	4.4134E-02	9.63E-07	7.9003E-03	5.80E-07	5.19E+08	−0.64	0.97	+2.15	0.55	+2.48	0.23
GR04023a@1	4.4149E-02	3.86E-06	7.8888E-03	1.84E-06	1.09E+08	−0.30	0.99	+0.68	0.70	+0.84	0.50
GR04023b@1	4.4197E-02	1.35E-06	7.8981E-03	6.62E-07	4.90E+08	+0.78	0.98	+1.87	0.55	+1.46	0.24
GR04023c@1	4.4191E-02	1.59E-06	7.8973E-03	7.29E-07	3.77E+08	+0.65	0.98	+1.77	0.56	+1.43	0.26
GR04023c@2	4.4188E-02	1.36E-06	7.8968E-03	7.36E-07	4.71E+08	+0.59	0.98	+1.70	0.56	+1.40	0.26
GR04023d@1	4.4323E-02	1.47E-06	7.9095E-03	7.90E-07	3.89E+08	+3.64	0.98	+3.31	0.56	+1.43	0.27
GR04023f@1	4.4403E-02	2.16E-06	7.9138E-03	1.35E-06	2.68E+08	+5.44	0.98	+3.86	0.63	+1.04	0.39

*Grain spot names begin with the sample number and a letter for specific grains, followed by @number, which designates the spot number on that grain.

[†]The 2 σ errors for the delta-values are calculated as two times the quadratic of the internal and external errors. The external error is the reproducibility of the standards and dominates over the internal error.
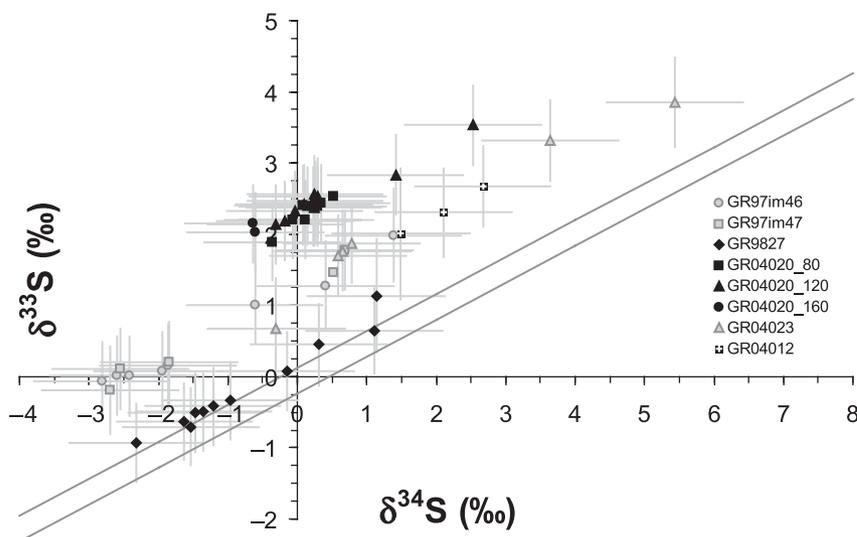
Fig. 3 Three-isotope plot of all sulfur isotope data (with 2 σ errors) collected on ISB metasediments for this study. Gray symbols represent data from quartz–garnet–biotite schists, while black symbols are for samples of BIF. The grey lines are MDF bands calculated from analyses on standards (λ = 0.518) and the space between them (~ ± 0.24‰, 2 σ) represents the field where MIF is irresolvable.

and +5.44‰. These results resemble the sulfur isotopic compositions previously reported for the *im*-series samples.

Banded iron-formation samples

Sulfides analysed from the three BIFs *GR9827*, *GR04012* and *GR04020* in Fig. 4 show variable sulfur isotope compositions. Sample *GR9827* has bands of large (>200 μM) pyrite grains within grunerite + magnetite and quartz bands. Subhedral to anhedral pyrites have $\Delta^{33}S$ values between +0.07 and +0.55‰, and $\delta^{34}S$ values between −2.31 and +1.14‰. One analysis on grain *GR9827e* provided a $\Delta^{33}S$ value of only +0.55‰, which represents small deviation from MDF, but this analysis had about a third of the ^{32}S average intensity of most other analysed pyrite and thus has a large uncertainty (Table 3). Samples of the Isua BIF *GR04020*-series were collected 80, 120 and 160 cm away from *GR97im23* and no significant trends in $\delta^{34}S$ or $\Delta^{33}S$ were observed between these samples (Fig. 3). The ranges of $\delta^{34}S$ and $\Delta^{33}S$ values for the *GR04020* samples are between −0.64 and +2.53‰ and between +2.07 and +2.47‰, respectively, which reproduces the data reported for *GR97im23* with $\delta^{34}S$ between +0.01 and +2.22‰ and $\Delta^{33}S$ between −0.25 and +2.02‰ (Mojzsis *et al.*, 2003). Minor variations in $\delta^{34}S$ (~3‰) may have been acquired from local factors at the time of deposition or post-depositional processes. However, to validate a primary depositional feature vs. alteration would require detailed analysis of intraband compared to interband variations in multiple sulfur isotopes. Our BIF sample *GR04012* contained few sulfides suitable for SIMS analysis. The two pyrrhotite grains sufficiently large to be analysed by ion microprobe appear to have been partly oxidized by later fluids, which left Fe-oxide coatings along cracks within grains (Fig. 4). Such oxidation is considered responsible for the low ^{32}S average intensities on these grains, and therefore the elevated errors on $\Delta^{33}S$ values (2 σ between

0.28 and 0.77). Nevertheless, measured $\Delta^{33}S$ values are between +1.21 and +1.28‰ and show well-resolved MIF sulfur isotopes despite the large associated errors.

DISCUSSION

Metamorphism and sulfide grain morphology in the ISB supracrustals

Although not quantified, the crystal habit of analysed sulfides from the ISB rocks in this study varies from anhedral to subhedral–euhedral and likely reflects differing degrees of metamorphic recrystallization of the amphibolite facies volcanosedimentary assemblage. Analysis of BSE and reflected light images failed to establish any obvious relation between sulfur isotopic composition and grain shape and/or size. Rounded sulfides may be of detrital origin if it could be established that they occur with other characteristic detrital minerals, but contributions from heavy mineral detritus is unlikely for the rocks types selected for this study (BIFs and fine-grained pelitic schists). Controls on sulfide morphology depend on a variety of factors, but rounded shapes in these rocks are more likely to be acquired via *in situ* growth and modification of crystal habit during one or more metamorphic episodes. An irregular texture is seen in reflected light images of polished sulfide surfaces in samples *GR9827*, *GR97im46*, *GR97im47* and *GR04023* (Figs 2 and 4), which likewise may be attributable to mode of recrystallization. Comparison of BSE and transmitted/reflected light images shows that the irregular textures represent different crystal faces and are not silicate or other inclusions. However, associations of Fe-oxides with sulfides are common in these rocks and occur as rims, parallel fractures, alteration zones along cracks and within grains (Figs 2 and 4). We consider postcrystallization oxidation and recent sulfide weathering as responsible for these features.
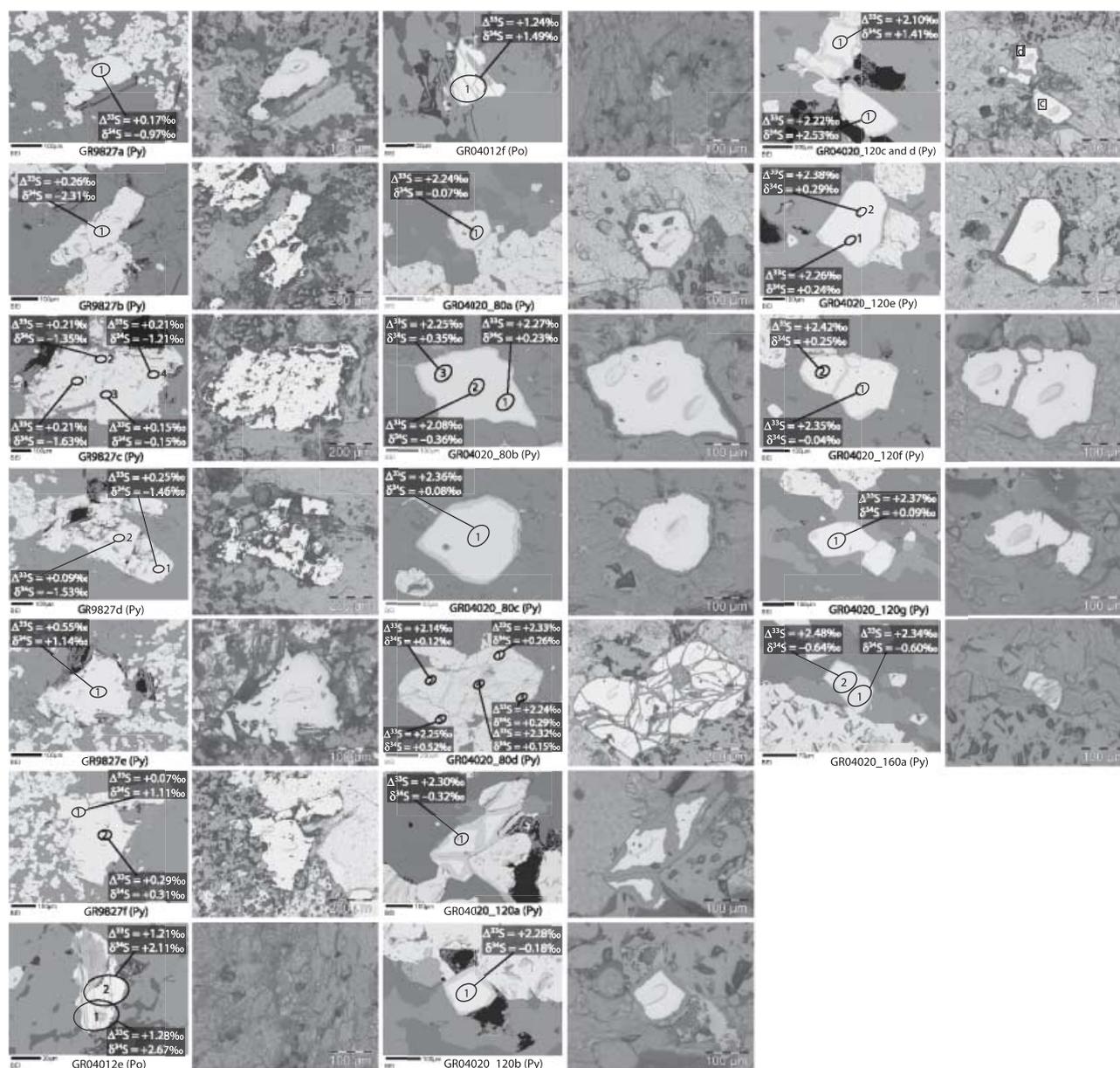
Fig. 4 Three sets of columns of backscattered electron images (left columns) and transmitted/reflected light images (right columns) of sulfides analysed from BIF samples *GR9827, GR04012* and *GR04020-series*. Ion microprobe spots are shown along with the measured $\delta^{34}S$ and $\Delta^{33}S$ values.

BSE and transmitted/reflected light images did not show any evidence for sulfide overgrowths on pre-existing sulfide cores. Based on this analysis, we conclude that arguments based on sulfide morphology alone are weak criteria to assess the authigenic-sedimentary origin (sulfide crystallized *in situ* from sedimentary sulfur) of sulfide grains in amphibolite facies rocks.

Mass-independent sulfur isotopes in high-grade sedimentary rocks from Isua

Metasedimentary units from the ISB preserve a small range of $^{34}S/^{32}S$ compositions. Our expanded data set is completely consistent with a compilation of published $\delta^{34}S$ and $\Delta^{33}S$ values as provided in Figs 5 and 6. Taken as a whole, the maximum range of published $\delta^{34}S$ data for sulfides compiled for the ISB ($n = 161$) is now found to be between −3.1 and +5.8‰ and for reported $\Delta^{33}S$ data ($n = 99$) is between −0.87 and +3.41‰. Because metamorphism only slightly fractionates sulfur isotopes during equilibrium and/or kinetic reactions that follow MDF rules, the range of reported $\Delta^{33}S$ is considered a robust indicator of mass-independent fractionation captured from the pre-3.77 Ga atmosphere. We wish to emphasize that in the interpretation of multiple sulfur isotope data, near-zero $\Delta^{33}S$ values do not necessarily imply high

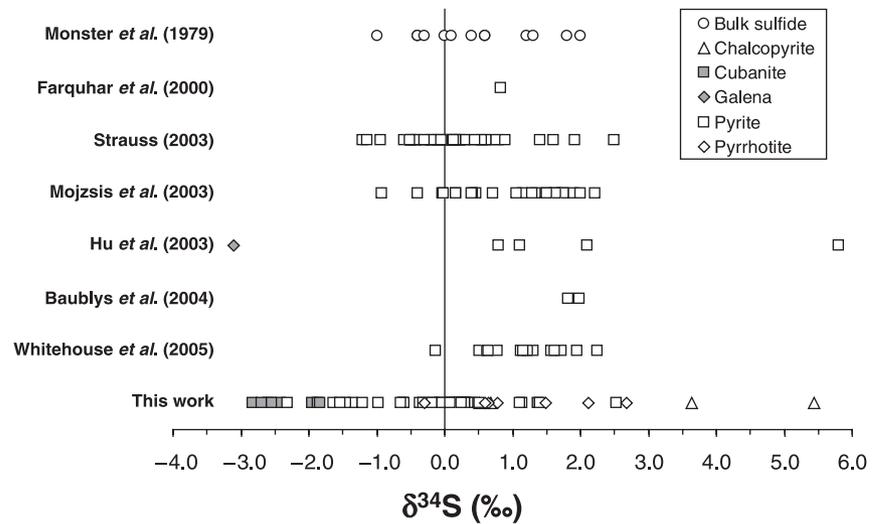**Fig. 5** Compilation of new and published δ^{34}S data ($n = 161$) for various sulfide phases in metasedimentary rocks from the Isua Supracrustal Belt.
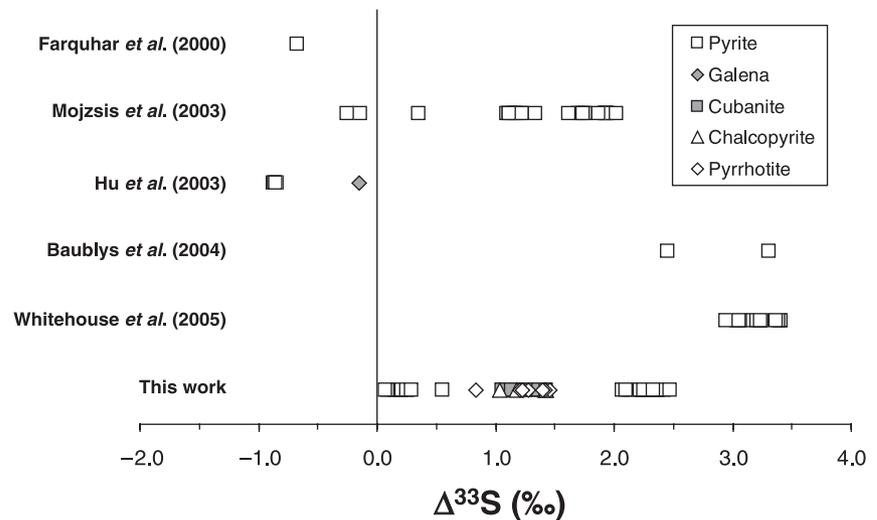

Fig. 6 Compilation of new and published Δ^{33}S data ($n = 99$) for various sulfide phases in metasedimentary rocks from the Isua Supracrustal Belt.

levels of atmospheric O_2 at time of deposition as advocated by some workers (Ohmoto *et al.*, 2006). MIF sulfur can be diluted, even to elimination, by fluids that contain MDF sulfur. If one were to propose that MIF sulfur isotopes were absent at any time during deposition of sulfur aerosols in the Archean, the claim would require other independent lines of evidence such as a combined data set of δ^{34}S values, mode of occurrence, sulfide composition and/or grain morphology that unambiguously point to a purely sedimentary source of sulfur (Papineau *et al.* submitted). Sample *GR9827* has large pyrite grains with positive Δ^{33}S values that fall on or slightly outside the 'normal' MDF band in Fig. 3. A range of ~3.4‰ in δ^{34}S values for *GR9827* is more simply explained by kinetic fractionation related to high-temperature metamorphism and isotopic equilibration processes. Interpretation of the isotope data does not require metabolic processing of sulfur at time of formation. Multiple analyses on grains *GR9827c* and *GR9827d* failed to show significant

intragranular heterogeneity or resolvable zonation in δ^{34}S and Δ^{33}S. The data instead suggest that pyrite in *GR9827* crystallized from isotopically homogeneous metamorphic sulfidic fluids which likely assimilated a mixture of MDF (dominant) and MIF (subordinate) sulfur isotopes during its migration.

The preservation of MIF sulfur isotopes in samples of undoubtedly marine sedimentary origin indicates atmospheric photochemical reactions on sulfur gases in the absence of oxygen. However, it appears that sulfur with MIF isotopes incorporated in sedimentary rocks from one area may leach in metamorphic fluids and be remobilized elsewhere. Chalcopyrite and cubanite grains from quartz lenses in metapelites *GR97im46* and *GR97im47* have Δ^{33}S values between +1.06 and +1.43‰ and δ^{34}S between −2.82 and +1.38‰. These results are similar to the ranges sulfur isotope ratios of pyrites in the quartz–biotite matrix reported from sample *GR97im43* collected from the same outcrop (Mojzsis *et al.*, 2003). The

Fig. 7 Qualitative illustration of the availability of oxygen and sulfate with the interpreted levels of respiration in the atmosphere–hydrosphere system at Isua time, during the Mid-Archean and during the Palaeoproterozoic transition (between 2.5 and 2.0 Ga).

data suggest that some sulfur in the original sedimentary rock was remobilized by fluids that also carried Cu, later to crystallize in close proximity as Cu-Fe-sulfides in quartz lenses. Alternatively, this could indicate that the source of sulfur came from an undetermined location and that all the sulfur in the *im*-series was remobilized during metamorphism. However, we favour the first interpretation because MIF in *GR97im43* occurs only in anhedral pyrite distributed parallel to schistosity and embedded within a dense phyllosilicate matrix, in which cubanite and chalcopyrite were absent (Mojzsis *et al.*, 2003). Moreover, analyses of chalcopyrite and pyrrhotite from the quartz-garnet-biotite schist *GR04023* collected along strike ~2 km south of the *im*-series showed an analogous range of $\Delta^{33}S$ and $\delta^{34}S$ values. These sulfides may have been influenced by metamorphic fluids, but their isotopic composition is in agreement with a sedimentary source of sulfur. Three samples from this outcrop and another collected from the same unit close to the locality of *GR04023* have been analysed for their nitrogen content and isotopic composition. Ammonium concentrations in biotite separates from samples *GR97im46*, *GR97im47* and *GR9817* vary between 233 and 512 p.p.m., consistent with a sedimentary source of nitrogen, possibly from the decay of organic matter at time of sedimentation (Papineau *et al.*, 2005b). Linking these observations back to the sulfur isotope data reported here, it seems that the small range of $\delta^{34}S$ values in these metapelites (including sulfur remobilized in quartz lenses) can be most simply explained by kinetic and isotopic equilibration processes rather than by biological fractionation of sulfur isotopes.

From the point of view of environmental chemistry, these coupled observations are entirely consistent with an anoxic atmosphere at 3.8 Ga and sulfur isotope data in Isua metasediments suggest low concentrations of dissolved seawater sulfate and atmospheric oxygen as illustrated in Fig. 7. If so, it is interesting to consider that the Eoarchean oceans would have been severely limited in many oxidants necessary for various respiration pathways and therefore could have been populated mainly by carbon-fixing autotrophs as suggested by ^{13}C-depleted graphite particles reported from Isua (Mojzsis *et al.*,

1996; Rosing, 1999; Ueno *et al.*, 2002). A point worthy of further exploration is whether the low abundance of oxidants in early Earth environments may not have been conducive to an extensive biosphere and/or to metabolically diverse microbial communities.

Possible variations in $\Delta^{33}S$ and $\delta^{34}S$ in sulfides from a finely laminated Isua BIF were investigated in ~2 m of fresh outcrop. Instead of preserving heterogeneous values that change 'stratigraphically' up-section in this unit, samples *GR04020-80*, *GR04020-120* and *GR04020-160* have homogeneous $\delta^{34}S$/ $\Delta^{33}S$ comparable to sample *GR97im23* reported in Mojzsis *et al.* (2003). Multiple analyses on individual pyrite grains also show homogeneous sulfur isotopic compositions. This suggests limited influence of metamorphic fluids subsequent to formation and a simple sulfur cycle dominated by (anoxic) atmospheric deposition of mass-independently fractionated reduced (S^0, S_8) sulfur aerosols at the time of formation. Based on our results thus far for ISB metasedimentary rocks (Fig. 5), it is not obvious from the isotopes that elemental sulfur from aerosol deposition was exploited by elemental sulfur reducers. The $\Delta^{33}S$ values measured in *GR04020* samples vary between +2.07 and +2.47‰, which is of comparable magnitude to other BIFs from Isua with reported $\Delta^{33}S$ values from +2.94 and +3.41‰ (Whitehouse *et al.*, 2005). Finally, three analyses on two partially oxidized pyrrhotite grains in BIF sample *GR04012* show relatively homogeneous sulfur isotopic composition with $\Delta^{33}S$ values slightly lower than in *GR04020* samples. We propose that subtle differences in sulfur isotopic composition between BIF units at Isua could have arisen from local factors such as different sources of sulfur at the time of deposition. These observations deserve further detailed investigations.

CONCLUSIONS

Sulfur isotopes in Early Archean sedimentary rocks are robust tracers of atmospheric redox chemistry, sulfur metabolisms and environmental conditions. Our 54 new ion microprobe $\Delta^{33}S$ analyses on sulfides reported here from metasediments of the ISB in West Greenland were measured with a technique that preserves petrographic context and enables direct evaluation of the sources of sulfur and elucidation of post-depositional isotopic disturbances. Data demonstrate that isotopic dilution of MIF signatures occurs during metamorphism with sulfide-rich fluids. Depending on the extent of mixing of MDF and MIF sulfur isotopes either during deposition or by later fluid infiltrations, any deviation from the MDF band can be obscured or erased. We documented remobilization of MIF sulfur isotopes in cubanite and chalcopyrite from quartz lenses in metapelites, which most likely precipitated with quartz veinings in these rocks. However, we surmise that the source of remobilized MIF sulfur probably came from nearby sedimentary rocks and that it is possible for MIF sulfur to migrate over short distances. Transport of MIF

in fluids over longer distances cannot be excluded, but isotopic dilution by MDF sulfur from intervening metaigneous lithologies would likely erase or obscure atmospheric signatures.

Our sulfur isotope data collected from rocks of sedimentary origin from the ISB suggest that the marine realm in the Eoarchean had low concentrations of dissolved sulfate and oxygen. Molecular phylogeny studies hint that some sulfur metabolisms evolved very early in the history of life, but as yet we find no convincing geochemical evidence to support this hypothesis for Isua time. The characteristic range of sulfur isotope ratios by MSR appears to be absent in ISB rocks. The earliest evidence put forward for MSR at time of formation is a suite of $\delta^{34}S$ values for microscopic pyrite grains embedded in 3.47 Ga barite from North Pole, Western Australia (Shen *et al.*, 2001). Most (>90%) $\Delta^{33}S$ values of sulfides reported from Eoarchean sedimentary rocks from Isua are positive (^{33}S enriched). This is interpreted to indicate the separation of sulfur reservoirs during atmospheric mass-independent fractionation processes, where reduced or neutral sulfur species produced by photochemical reactions carried positive $\Delta^{33}S$ values and dominated the source of aerosols to the Archean ocean. Although available for microbial elemental sulfur reduction, we find no evidence that this sulfur was metabolized. We anticipate that if sulfate of demonstrably primary origin from Isua rocks is found, it should preserve negative $\Delta^{33}S$ values with a relatively small range in $^{34}S/^{32}S$.

ACKNOWLEDGEMENTS

REFERENCES

Anthony JW, Bideaux RA, Bladh KW, Nichols MC (1990) *Handbook of Mineralogy*, Vol. I. Mineral Data Publishing, Tucson, Arizona.

Baublys KA, Golding SD, Young E, Kamber BS (2004) Simultaneous determination of $\delta^{33}S_{V-CDT}$ and $\delta^{34}S_{V-CDT}$ using masses 48, 49 and 50 on a continuous flow isotope ratio mass spectrometer. *Rapid Communications in Mass Spectrometry* **18**, 2765–2769.

Canfield DE (1998) A new model for Proterozoic ocean chemistry. *Nature* **396**, 450–453.

Canfield DE, Raiswell R (1999) The evolution of the sulfur cycle. *American Journal of Science* **299**, 697–723.

Detmers J, Brüchert V, Habicht KS, Kuever J (2001) Diversity of sulfur isotope fractionations by sulfate-reducing Prokaryotes. *Applied and Environmental Microbiology* **67**, 888–894.

Dymek RF, Klein C (1988) Chemistry, petrology, and origin of banded iron-formation lithologies from the 3800 Ma Isua supracrustal belt, West Greenland. *Precambrian Research* **39**, 247–302.

Farquhar J, Bao H, Thiemens MH (2000) Atmospheric influence of Earth's earliest sulfur cycle. *Science* **289**, 756–758.

Fedo CM, Myers JS, Appel PWU (2001) Depositional setting and paleogeographic implications of Earth's oldest supracrustal rocks, the >3.7 Ga Isua Greenstone belt, West Greenland. *Sedimentary Geology* **141**, 61–77.

Friend CRL, Nutman AP (2005) Complex 3670–3500 Ma orogenic episodes superimposed on juvenile crust accreted between 3850 and 3690 Ma, Itsaq Gneiss Complex, southern West Greenland. *Journal of Geology* **113**, 375–397.

Friend CRL, Nutman AP, Bennett VC (2002) Protolith of the 3.8–3.7 Ga Isua greenstone belt, West Greenland – comment. *Precambrian Research* **117**, 145–149.

Greenwood JP, Mojzsis SJ, Coath CD (2000) Sulfur isotopic composition of individual sulfides in Martian meteorites ALH84001 and Nakhla: Implications for crust-regolith exchange on Mars. *Earth and Planetary Science Letters* **184**, 23–35.

Habicht KS, Gade M, Thamdrup B, Berg P, Canfield DE (2002) Calibration of sulfate levels in the Archean ocean. *Science* **298**, 2372–2374.

Hu G, Rumble D, Wang PL (2003) An ultraviolet laser microprobe for the in situ analysis of multisulfur isotopes and its use in measuring Archean sulfur isotope mass-independent anomalies. *Geochimica et Cosmochimica Acta* **67**, 3101–3117.

Kretz R (1983) Symbols for rock-forming minerals. *American Mineralogist* **68**, 277–279.

Mojzsis SJ, Arrhenius G, McKeegan KD, Harrison TM, Nutman AP, Friend CRL (1996) Evidence for life on Earth before 3800 million years ago. *Nature* **384**, 55–59.

Mojzsis SJ, Coath CD, Greenwood JP, McKeegan KD, Harrison TM (2003) Mass-independent isotope effects in Archean (2.5–3.8 Ga) sedimentary sulfides determined by ion microprobe analysis. *Geochimica et Cosmochimica Acta* **67**, 1635–1658.

Monster J, Appel PWU, Thode HG, Schidlowski M, Carmichael CM, Bridgwater D (1979) Sulfur isotope studies in early Archaean sediments from Isua, West Greenland: implications for the antiquity of bacterial sulfate reduction. *Geochimica et Cosmochimica Acta* **43**, 405–413.

Myers JS (2001) Protoliths of the 3.8–3.7 Ga Isua greenstone belt, West Greenland. *Precambrian Research* **105**, 129–141.

Myers JS (2002) Protolith of the 3.8–3.7 Ga Isua greenstone belt, West Greenland – reply. *Precambrian Research* **117**, 151–156.

Nutman AP, Allaart JH, Bridgwater D, Dimroth E, Rosing MT (1984) Stratigraphic and geochemical evidence for the depositional environment of the Early Archaean Isua Supracrustal Belt, southern West Greenland. *Precambrian Research* **25**, 365–396.

Nutman AP, McGregor VR, Friend CRL, Bennett VC, Kinny PD (1996) The Itsaq Gneiss Complex of southern West Greenland: the world's most extensive record of early crustal evolution (3900–3600 Ma). *Precambrian Research* **78**, 1–39.

Nutman AP, Friend CRL, Barker SLL, McGregor VR (2004) Inventory and assessment of Palaeoarchaean gneiss terrains and detrital zircons in southern West Greenland. *Precambrian Research* **135**, 281–314.

Ohmoto H, Watanabe Y, Ikemi H, Poulson SR, Taylor BE (2006) Sulfur isotope evidence for an oxic Archaean atmosphere. *Nature* **442**, 908–911.

Ono S, Eigenbrode JL, Pavlov AA, Kharecha P, Rumble D, Kasting JF, Freeman KH (2003) New insights into Archean sulfur cycle from mass-independent sulfur isotope records from

the Hamersley Basin, Australia. *Earth and Planetary Science Letters* **213**, 15–30.

Papineau D, Mojzsis SJ, Coath CD, Karhu JA, McKeegan KD (2005a) Multiple sulfur isotopes of sulfide from sediments in the aftermath of Paleoproterozoic glaciations. *Geochimica et Cosmochimica Acta* **69**, 5033–5060.

Papineau D, Mojzsis SJ, Karhu JA, Marty B (2005b) Nitrogen isotopic composition of ammoniated phyllosilicates: case studies from Precambrian metamorphosed sedimentary rocks. *Chemical Geology* **216**, 37–58.

Papineau D, Mojzsis SJ, Schmidt AK (in review) Multiple sulfur isotopes from Paleoproterozoic Huronian interglacial sediments and the rise of atmospheric oxygen.

Pinti DL, Hashizume K, Matsuda J (2001) Nitrogen and argon signatures in 3.8–2.8 Ga metasediments: clues on the chemical state of the Archean ocean and the deep biosphere. *Geochimica et Cosmochimica Acta* **65**, 2301–2315.

Rose NM, Rosing MT, Bridgwater D (1996) The origin of metacarbonate rocks in the Archaean Isua Supracrustal Belt, West Greenland. *American Journal of Science* **296**, 1004–1044.

Rosing MT (1999) ^{13}C-depleted carbon microparticles in >3700-Ma sea-floor sedimentary rocks from West Greenland. *Science* **283**, 674–676.

Rosing MT, Rose NM, Bridgwater D, Thomsen HS (1996) Earliest part of Earth's stratigraphic record: a reappraisal of the 3.7 Ga Isua (Greenland) supracrustal sequence. *Geology* **24**, 43–46.

Schidlowski M (1988) A 3800-million-year isotopic record of life from carbon in sedimentary-rocks. *Nature* **333**, 313–318.

Schidlowski M, Hayes JM, Kaplan IR (1983) Isotopic inference of ancient biochemistroes: carbon, sulfur, hydrogen, and nitrogen. In: *Earth's Earliest Biosphere* (ed. Schopf JW). Princeton University Press, Princeton, New Jersey, pp. 149–186.

Shen Y, Buick R, Canfield DE (2001) Isotopic evidence for microbial sulphate reduction in the early Archaean era. *Nature* **410**, 77–81.

Stetter KO, Gaag G (1983) Reduction of molecular sulphur by metanogenic bacteria. *Nature* **305**, 309–311.

Strauss H (2003) Sulphur isotopes and the early Archaean sulphur cycle. *Precambrian Research* **126**, 349–361.

Ueno Y, Yurimoto H, Yoshioka H, Komiya T, Maruyama S (2002) Ion microprobe analysis of graphite from ca. 3.8 Ga metasediments, Isua supracrustal belt, West Greenland: relationship between metamorphism and carbon isotope composition. *Geochimica et Cosmochimica Acta* **66**, 1257–1268.

Whitehouse MJ, Kamber BS, Fedo CM, Lepland A (2005) Integrated Pb- and S-isotope investigation of sulphide minerals from the early Archaean of southwest Greenland. *Chemical Geology* **222**, 112–131.

van Zuilen MA, Lepland A, Arrhenius G (2002) Reassessing the evidence for the earliest traces of life. *Nature* **418**, 627–630.

van Zuilen MA, Mathew K, Wopenka B, Lepland A, Marti K, Arrhenius G (2005) Nitrogen and argon isotopic signatures in graphite from the 3.8-Ga-old Isua Supracrustal Belt, Southern West Greenland. *Geochimica et Cosmochimica Acta* **69**, 1241–1252.